Article

An Experimental Investigation of the Thermal and Economic Performance of PCM-Embedded Hybrid Water Heater under Saharan Climate

Sidi Mohammed El Amine Bekkouche [1,] *, Rachid Djeffal [1], Mohamed Kamal Cherier [1], Maamar Hamdani [1], Zohir Younsi [2], Saleh Al-Saadi [3] and Zaiani Mohamed [1]

1. Unité de Recherche Appliquée en Energies Renouvelables, URAER, Centre de Développement des Energies Renouvelables, CDER, 47133, Ghardaïa, Algeria
2. FUPL, Hautes Etudes d'Ingénieur (HEI), LGCgE (EA 4515), Rue de Toul, F-59000 Lille, France. Univ. Artois, Laboratoire Génie Civil & Geo-Environnement LGCgE-EA 4515, Technoparc Futura, F-62400 Béthune, France
3. Department of Civil and Architectural Engineering, Sultan Qaboos University, PO Box 33, Postal Code 123, Oman

* Correspondence: author: smabekkouche@gmail.com

Abstract. The solar water heater must be integrated into future residential buildings as the main energy source, which will subsequently reduce the energy cost of water heating. An original configuration for efficient Domestic Hot Water "DHW" storage tank is developed and experimentally evaluated under Saharan climate. This novel DHW configuration includes a hybrid (solar and electric) energy system with a flat plate solar collector coupled with an electric heater. Additionally, phase change material "PCM" mixture that is composed of paraffin wax and animal fat with a melting temperature between 35.58°C and 62.58°C and latent heat between 180 and 210 kJ/kg is integrated into this novel tank configuration. The experimental results indicated that hot water production by using latent heat storage could be economically attractive. In this proposed configuration, one liter of hot water may cost around 0.1362 DZD/liter (i.e., 0.00096 US$/liter) compared to 0.4431 DZD/liter for the conventional water heater, an average energy cost savings of 69.26%. On a yearly basis, the average energy cost savings may reach up to 80.25% if optimal tilt for the solar collector is adopted on a monthly basis. The flat plate collector may be vulnerable to convective heat transfer, and therefore, other solar collectors such as vacuum tube collectors may provide enhanced energy performance.

Keywords: hybrid DHW system; water heater; PCM; melting temperature; latent heat storage; produced water cost

1. Introduction

According to the Ecological Transition Agency (ADEME), the domestic hot water (DHW) of a French household is a major energy consumption item since it represented, in 2012, 12.1% of the average energy consumption, against 61.3% for heating and 7% for cooking **[1]**. To determine the energy consumption of the electric water heater storage tank, several factors must be taken into account: the capacity of the hot water tank, the family composition, and hot water consumption patterns. Regardless of the tank volumes (i.e., 50 liters, 150 liters, or

Preprints (www.preprints.org) | NOT PEER-REVIEWED | Posted: 6 December 2022 doi:10.20944/preprints202212.0095.v1

200 liters), the hot water tank consumes a relatively high amount of electricity. A few daily actions can be enough to reduce hot water consumption, but the choice of the type of water heater also impacts this consumption and, therefore, the energy consumption. The electric storage heater with the joule effect is sometimes the most widely used electric DHW production system **[2]**. It is the easiest and most straightforward approach to producing hot water in the housing sector. It consists of a corrosion-protected tank, an electrical resistance, and a thermostat to regulate the water temperature inside the tank. The content is spontaneously replaced as the produced hot water is consumed. The focus of the conducted work in an international project **[3]** was on the information likely to enlighten the design of complete cartography accompanied by a comparative study of the different water heaters. The scoping study covered residential water heaters such as electric, gas, solar water heaters, and tank types in several countries and regions, including Australia, Brazil, Canada, China, European Union, India, South Korea, and the United States. There are three main types of water heaters: electric, gas, and renewable energy heaters, as shown in Figure 1. Several essential criteria may be used to select among these types, including the economic, ecological, and energy performance **[4-8]**.

In South Africa, hot water is widely used for DHW and space heating. The water heating process requires a large amount of energy, estimated at 40% of the total energy **[9]**. This study also indicated that electric water heating is dominant in the country. According to Catherine et al. **[10]**, a typical middle-class residential building can consume on average about 11797 kWh/year, out of which 4259 kWh/year (~36.1%) is used for water heating. In the United States, the heating energy for DHW at the urban scale represents 17% **[11]**. Nearly 40% of buildings use electricity for water heating. This fraction differs significantly from state to state, with more than 80% of facilities in some states and less than 15% of others using electric storage tank water heaters.

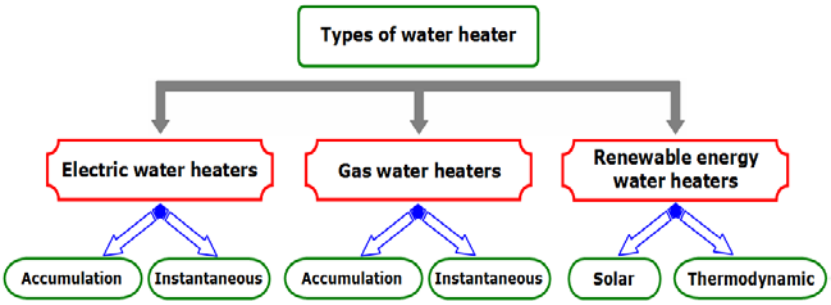

Figure 1. Main types of storage tank water heaters **[11]**.

The intensive use of electricity for heating has motivated some researchers **[12]** to propose solutions for energy savings. One effective solution was to control the electricity supply of water heaters during peak hours in residential buildings **[13]**. The thermal efficiency of storage type electric water heaters is affected by the control mechanism. In 2005, according to Jiang and Yang **[14-15]**, the number of water heating units in China was 72.7 per 100 urban households. Gas, electric, and solar water heaters accounted for 57.4%, 31.3%, and 11.3%, respectively. Electric water heaters have a significant share of the Chinese market due to low installation costs and product profitability, but it was also noted that its design lacks innovation. The main topics

 doi:10.20944/preprints202212.0095.v1

of existing studies focused on the improvement of energy efficiency, availability, and quality of product installation services **[16]**. In contrast to the other studies on electric water heaters, which have shown a declining trend, there has been a significant increase in studies on air and solar water heaters between 1998 and 2014 **[16]**. Tan et al. **[17]** have proposed a practical method to improve the storage type electric water heater by integrating an intelligent control system driven by a single chip microcomputer for safe operations. Dong **[18]** has conducted a correlation analysis on factors affecting user satisfaction with electric water heaters.

On the other hand, the most important function of the storage-type electric water heater is to heat the water using electrical energy and store it for later use. Electrical energy is supplied to the electrical resistive elements inside the storage-type water tank. Current flows through the elements to create heat, which generates thermal energy that will then be exchanged with the surrounding water. Unfortunately, this heating process requires significant energy that has become unaffordable in recent years. Therefore, alternative heating technologies are indisputable and must be utilized to reduce the overall operating costs. As a result of these financial and technical circumstances, renewable energy must be used to reduce energy consumption and the associated energy cost in the residential sector. Solar or hybrid water heaters can be an effective solution to overcome the expensive energy cost. According to the literature **[19-30]**, the choice generally focuses on the forced circulation solar water heater due to its considerable strength compared to the thermosiphon solar water heater. Its advantage is its storage water tank which can be positioned almost anywhere, especially below the sensors.

In Algeria, electricity is generated using open-cycle gas turbines, which is considered an expensive method for electrical generation, his government subsidies the electricity which led to an excessive energy use. More than 72% of the produced energy is consumed in the southern region of Algeria, while the rest is consumed in the coastal and highland areas. For typical housing in Algeria, water heating consumes between 20% and 30%, mainly using electricity **[31]**. One approach to reducing the electrical water heating demand is to use solar energy. Due to the variability and the intermittent nature of solar radiation, thermal energy storage using phase change materials (PCMs) has shown the potential to elongate the use of solar energy as well as flatten the supply of energy. In addition, in the last years, electric storage water heaters have been subjected to technical challenges such as low heating rates and inconsistent temperature control of the stored water. These operational problems have resulted in insufficient hot water production and irregular hot water supply, which could create inconvenience to users.

This article reports an experimental analysis on PCM embedded flat plate solar collector coupled with electric heater. This study proposes a novel design configuration for an active water heater embedded with PCM that can provide a reliable design solution. The system is hybrid which consists of a flat plate solar collector and an electric heater as a backup heat source. In this work, the thermophysical properties of a newly proposed PCM are characterized. Then, the integration mechanism with the active water heater is illustrated. The comparison of the performance of this hybrid energy source system, which consists of a conventional flat plate-collector and a PCM storage

 doi:10.20944/preprints202212.0095.v1

tank, based on energy consumption has been widely discussed. The analysis was based on a single day experimental data corresponding to only a single test. The renewal of a comparative test corresponding to the same case was based on experiments carried out on another day similar to the previous one. The only and main objective is therefore to greatly reduce the amount of primary energy needed for the domestic use of hot water. This conducted research was confined to the measurement of the power consumption by the entire energy systems and the average temperature in the storage tanks according to their equivalent heat loss coefficients (U-value). The stated objectives therefore not concerned with determining the thermal performance of the flat water collector or the variation of the water inlet and outlet temperatures. This important issue was already solved in many distinguished contributions **[32-35]** and served as further contributions. In addition to the technical feasibility, the economic feasibility is also conducted for this new PCM-integrated hybrid water heater. Several parameters are determined at various thermostat setpoints, including produced hot water volume, a substantial gain in production terms, corresponding electric bills, the unit price corresponding to a produced volume at 50°C, and the financial gain. Furthermore, the results of this work cannot be compared with others studies from the literature libraries because of this new PCM sample (homogeneous and completely odorless) which does not exist in the bibliographic references.

2. Material and method

A newly hybrid (i.e., solar and electrical) water heater is proposed for integration into residential buildings, consequently reducing the energy cost of water heating, mainly for domestic use. The installation is an active solar thermal system, consisting of a storage tank, pipes and pumps. Components, processes and effects that are part of the system are broken down into sub-systems. The interactions between these components, which are in response to climatic variations and energy requirements, determine the amount of useful energy that will be delivered by the system. For example, the only specific characteristics related the sensor cannot be used directly to determine the produced energy since this depends on the operating sensor temperature which in turn depends on the storage temperature. Functionally, however, the active solar system can be represented as shown in Figure 2.

For the capture phase, a glazed flat collector of acceptable optical quality (transparent or absorbent materials) has been set up, which converts solar radiation into heat with an efficiency that reaches up to nearly 69.5% **[32]**. The collected sun's energy will be transformed into heat and then transferred by forced circulation of the heat transfer fluid (water) in the pipes to the storage system via a manually controlled circulation pump. The volumetric flow rate was set at 130 liters per hour. The used pipes are made of galvanized steel characterized by a low heat conduction rate and protected with thermal insulation against thermal losses and bad weather.

Preprints (www.preprints.org) | NOT PEER-REVIEWED | Posted: 6 December 2022 doi:10.20944/preprints202212.0095.v1

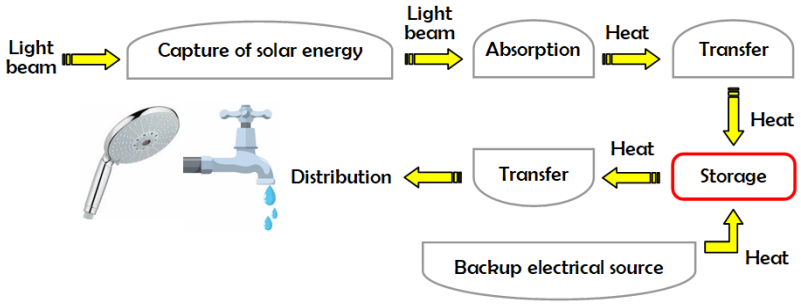

Figure 2. Functional representation of the hybrid energy system **[36]**

In most cases, solar energy cannot ensure all energy needs. To cope with unfavourable periods (winter, mid-season, long period of bad weather), additional energy will be needed. Thus, this storage unit is equipped with an individualized back-up device with direct distribution. This system design incorporates an electrical heating element as a backup energy source, as shown in Figure 3. In this work, the developed hybrid water heater is used as a test bench.

A flat plate solar collector is used to heat the water that flows in a hydraulic circuit connected to the storage tank. Solar radiations, symbolized by the yellow arrows in Figure 4, will partially be reflected ($R_{ref/glass}$), especially if the incident angle is sharp. Despite the excellent transparency of the glass, a small part of the received energy ($R_{1\ abs/glass}$) will be absorbed by the glass. The portion $R_{ref/abs}$ of the received radiation by absorber $R_{1\ abs/abs}$ will be re-radiated or transferred to the ambient air by convection shown as $R_{trans/glass}$ in the Figure 4. Another part $R_{2\ abs/glass}$ will be absorbed by the glass cover, and the rest $R_{2\ abs/abs}$ will return to the absorber. The hybrid water heater is installed on a rooftop of an office building at the Applied Research Unit in Renewable Energies, as shown in Figure 4. The racking system allows several inclinations which may be used to direct the flat plate solar collector to absorb the maximum amount of solar radiation. The metal absorber is coated with a dark and selective paint (black chrome) to maintain its physical (i.e., surface treatment, dilatation, etc.), thermal (i.e., conductivity, absorber-fluid connection, etc.), and hydraulic (i.e., pressure losses, fouling, purging, etc.) properties over time. The system was equipped with several protection features, including antifreeze, air oxidation, UV rays. The transparent layer is made of tempered glass. The absorber emits the reflected solar radiation, which promotes the greenhouse phenomenon. Thermal insulation is used to minimize thermal losses to the outside environment. The physical, the optical, and the thermo-physical characteristics are listed in Table 1. The system was commissioned without any noticeable water leaks.

Preprints (www.preprints.org) | NOT PEER-REVIEWED | Posted: 6 December 2022 doi:10.20944/preprints202212.0095.v1

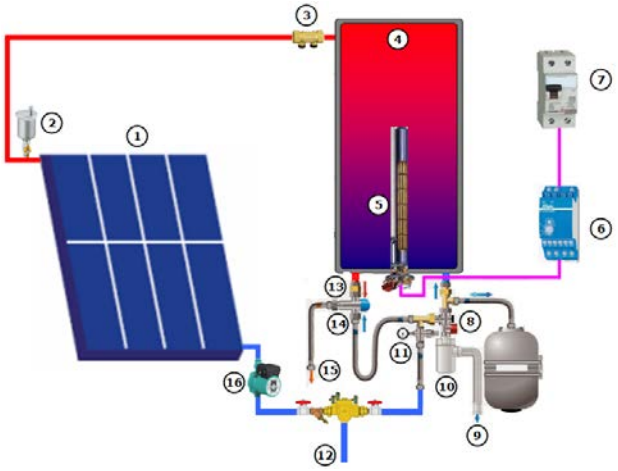

1. Water flat solar collector
2. Automatic air vent with shut-off valve
3. Check valve
4. Hot water storage tank with spiral heat exchanger
5. Electrical resistance with thermostat (key piece to monitoring and adjust the set temperature)
6. Electromechanical relay
7. Electrical circuit breaker, circuit breaker
8. Safety system
9. Evacuation
10. Siphon funnel
11. Pressure reducer
12. Domestic cold water, cold water supply
13. Domestic hot water
14. Thermostatic safety limiter
15. Mixed water
16. Circulator, recirculation pump

Figure 3. Schematic description of the test rig, hybrid solar/electric water heating system

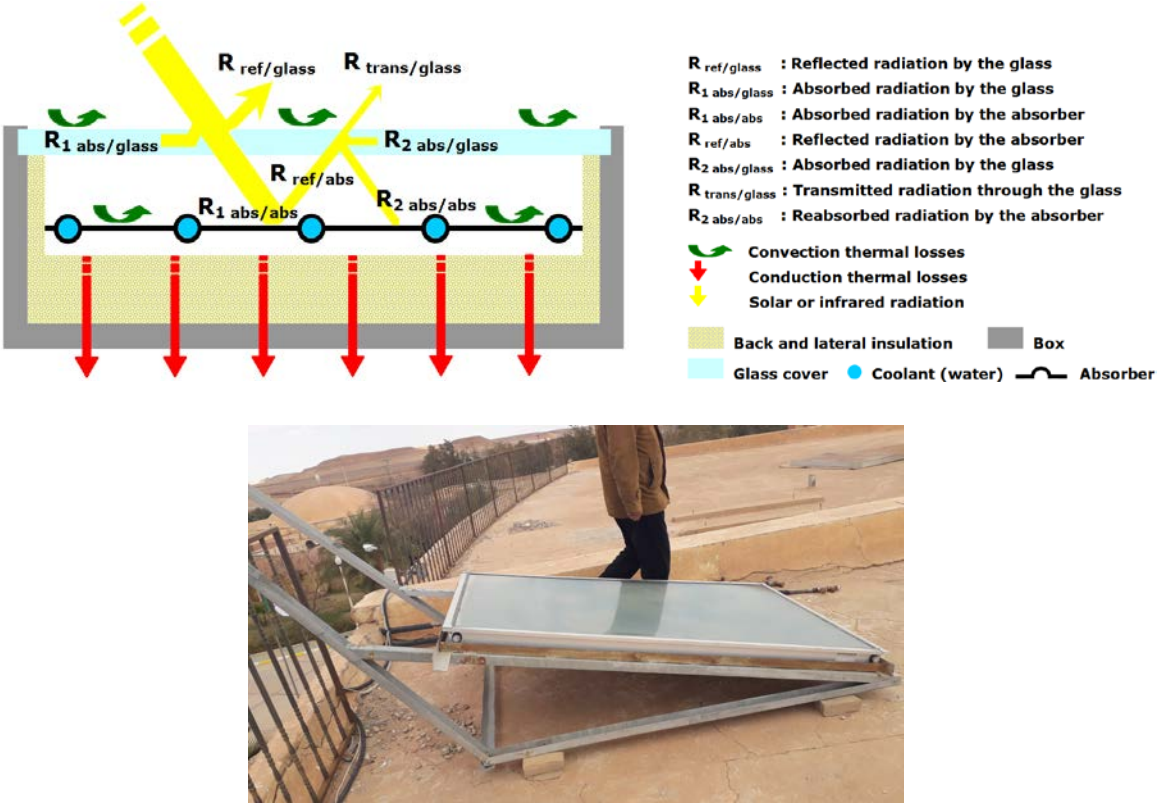

Figure 4. Descriptive image, schematic section, and operating principle of the solar water collector

Isothermal tanks are used for the storage of hot water in order to stabilize the water temperature. The integrated storage system is composed of the following:

- Two enameled storage tanks of 80-liters in parallelepiped form, equipped with well-dimensioned smooth tube heat exchangers (15 m length and 16 mm diameter) to ensure optimum performance, are used. The two storage tanks can be operated using two modes: either using electricity or hybrid using solar and electricity. Two main configurations of storage tanks were studied: a conventional storage tank (no PCM) and a PCM-embedded storage tank without insulation (i.e., high thermal losses). The PCM-embedded storage tank was then enhanced with thermal insulation, a design case that has low thermal losses, which represents an additional design

Preprints (www.preprints.org) | NOT PEER-REVIEWED | Posted: 6 December 2022 doi:10.20944/preprints202212.0095.v1

configuration. The three configurations are articulated in Table 2, which provides more details about the geometric and thermal properties of the storage tanks.

- Two copper electrical resistors, controlled by two encapsulated thermostats in direct contact with the stored fluid, are used. The thermostats' main task is to cut off the electrical supply of the resistor when the required temperature is reached.

Table 1. Description of the component elements, geometric, optical, and thermophysical properties of the solar water collector.

Component elements		Geometric properties	Optical and thermophysical properties
Galvanized Steel TRAY		Length : 2050 mm Width : 1275 mm Height : 90 mm Thickness : 3 mm Gross sensor area : 2.613 m²	/
Cover (micro prism glass)		Length : 1900 mm Width : 1200 mm Thickness : 3.5 mm	Transmittance coefficient : 0.87 Emissivity coefficient : 0.88 Glass reflectance factor : 0.09 Glass absorption factor : 0.03 Density : 2700 Kg/m³
Absorber (of copper)	Coated flat absorber	Width : 1200 mm Thickness : 0.2 m Net surface : 2.31 m²	Thermal conductivity : 389 W/m K Absorptivity : 0.92 Expansion coefficient : 1.65 Density : 8900 Kg/m3
	Coated absorber tubes	iameter of the main collector : 22 mm Tube diameter : 10 mm Thickness : 0.2 mm Space between tubes : 270 mm	Silver welding : minimum 30% silver Thermal conductivity : 389 W/m K Solder conductance : 35 W/m K Absorptivity : 0.92 Density : 8900 Kg/m³
Insulation		Back insulation : 4 cm rockwool	Thermal conductivity 0.038 W/m K Density 40 Kg/m³ Specific heat 840 J/kg °C Thermal diffusivity 11.9 10^{-7} m²/s
		Lateral insulation : 2 cm glass wool	Thermal conductivity : 0.036 W/m K Density : 40 Kg/m³ Specific heat : 840 J/kg °C Thermal diffusivity : 10.7 10^{-7} m²/s
Heat absorption medium (water)		/	Specific heat: 4180 J/kg °C Water density (Kg/m³) $-0.0038\ T^2 - 0.0505\ T + 1002.6$ Thermal conductivity (W/m K) $-9.87\ 10^{-6}\ T^2 + 2.238\ 10^{-3}\ T + 0.5536$ Dynamic viscosity (Kg/ms or Pa s) $(0.002\ T^2 - 0.3389\ T + 17.199)\ 10^{-4}$ T temperature in °C

- Two heat exchangers are devices that transfer heat in order to obtain the desired heating. Copper was selected because it is an excellent conductor of heat and has ideal thermal properties, especially its thermal conductivity. The manufacturing of a copper coil heat exchanger is simple and can be easily manipulated in the lab.

The safety system: this group of devices ensures the safety of the system. The safety system constantly monitors the temperature and

Preprints (www.preprints.org) | NOT PEER-REVIEWED | Posted: 6 December 2022 doi:10.20944/preprints202212.0095.v1

pressure of fluid inside the circulation loop. This system is set "open" if the water pressure exceeds 2 bars.

For space and water heating, a well-loaded hot water balloon undergoes a reduction in water temperature over time due to heat losses. Heat losses (Q) in storage tanks occur due to conductive heat transfer through the tank walls and other accessories and then transferred to the ambient air through convective heat transfer, which can be estimated using equation 1 **[37]**:

$$Q = U\ A\ (T_{Tank} - T_{Sur\text{-}Air}) \quad (1)$$

U: Overall heat transfer coefficient of the storage tank (W/K)
A: Total area of the tank wall (m²).
T_{Tank}: Temperature of the tank water (K).
$T_{Sur\text{-}Air}$: Temperature of the surrounding air (K).
Equation 1 can be simplified in the following form:

$$Q = \left(\frac{A_{Horizontal\ -walls}}{A} U_{Horizontal\ -walls} + \frac{A_{Side\ -walls}}{A} U_{Side\ -walls} \right) (T_{Tank} - T_{Sur\ -Air}) \quad (2)$$

$$Q = \left(\frac{A^2_{Horizontal\ -walls}}{A}\ U\ -value\ _{Horizontal\ -walls} + \frac{A^2_{Side\ -walls}}{A}\ U\ -value\ _{Side\ -walls} \right) (T_{Tank} - T_{Sur\ -Air}) \quad (3)$$

U-value is the thermal transmittance value given in Table 2 (W/K/m²).

$$U\ -value = \frac{1}{R_{si} + \sum_{i=1}^{i=n} R_i + R_{se}} \quad (4)$$

R_{si}, R_{se} represent, respectively, the internal and external surface thermal resistances (m² K/W).
R_i is defined as the thermal resistance of each layer (m² K/W)

Table 2. Specifications of the storage tanks

Properties			Conventional storage tank (High thermal losses)	PCM storage tank (High thermal losses)		PCM insulated storage tank (Low thermal losses)	
Capacity (L)			80	80		80	
Height H (cm)			51	51		59	
Length P (cm)			41	42		46	
width B (cm)			41	42		46	
Total area (m²)			1.17	1.21		1.36	
U-value (W/m² °C)	horizontal side	High	4.76	4.76		0.77	
		Low	7.14	7.14		0.82	
	lateral sides		2.86	PCM in liquid state 2.45	PCM in solid state 2.52	PCM in liquid state 0.67	PCM in solid state 0.68

The type of material and the outer layer thickness play a major role in the heat transfer process. All lateral sides of the tank were thermally insulated using 4 cm thick polystyrene insulation, which was selected due to its lower thermal conductivity (typically at 0.036 W/m.K). In order to characterize this process, several tests were conducted to measure the thermal losses from the three tank typologies. The ambient air temperature was varied together with the water temperature inside the tank. The thermal losses were calculated using equation 1, and the results are summarized in Table 3.

Preprints (www.preprints.org) | NOT PEER-REVIEWED | Posted: 6 December 2022 doi:10.20944/preprints202212.0095.v1

The thermal conductivity of the PCM mixture was measured by differential scanning calorimetry (DSC). According to the DSC results, the thermal conductivity was 0.215 W/m.K for the solid-state and 0.175 W/m.K for the liquid-state **[37, 38]**. The temperature gradient between the hot water tank and the ambient air temperature should be minimized. The water temperature has to be above the threshold temperature to eliminate bacteria such as legionella. The bacterium enters the body by inhalation and can cause atypical pneumonia, accompanied by fever with severe headache, chills, diarrhea, and difficulty breathing. If the bacterium spreads in a temperature range of 20 to 50°C, the ideal temperature for its development is 38°C. It no longer reproduces when the water temperature exceeds 50°C and dies above 70°C. The proliferation of Legionella bacteria in DHW systems is promoted by the biofilm's presence and mechanical deposits in which other bacteria live.

Table 3. Thermal losses through storage tanks (W)

Surrounding air temperature (°C)	Water temperature in the storage tank (°C)														
	Conventional storage tank					PCM storage tank					PCM insulated storage tank				
	40	50	60	70	80	40	50	60	70	80	40	50	60	70	80
12	7.38	10.01	12.65	15.29	17.92	7.15	9.71	12.09	14.61	17.13	1.79	2.42	3.09	3.74	4.38
14	6.85	9.49	12.12	14.76	17.39	6.64	9.20	11.59	14.11	16.62	1.66	2.30	2.97	3.61	4.26
16	6.32	8.96	11.60	14.23	16.87	6.13	8.69	11.08	13.60	16.12	1.53	2.17	2.84	3.48	4.13
18	5.80	8.43	11.07	13.70	16.34	5.62	8.18	10.58	13.10	15.62	1.40	2.04	2.71	3.35	4.00
20	5.27	7.91	10.54	13.18	15.81	5.11	7.66	10.08	12.59	15.11	1.28	1.91	2.58	3.22	3.87
22	4.74	7.38	10.01	12.65	15.29	4.60	7.15	9.57	12.09	14.61	1.15	1.79	2.45	3.09	3.74
24	4.22	6.85	9.49	12.12	14.76	4.09	6.64	9.07	11.59	14.11	1.02	1.66	2.32	2.97	3.61
26	3.69	6.32	8.96	11.60	14.23	3.58	6.13	8.56	11.08	13.60	0.89	1.53	2.19	2.84	3.48
28	3.16	5.80	8.43	11.07	13.70	3.07	5.62	8.06	10.58	13.10	0.77	1.40	2.06	2.71	3.35
30	2.63	5.27	7.91	10.54	13.18	2.55	5.11	7.56	10.08	12.59	0.64	1.28	1.93	2.58	3.22

This is particularly true for some poorly designed systems that lack a water circulation device. It is for this reason that the chosen volume of the storage tank has been retained in such a way that the temporary stagnation of the water and thus the "impasses" can be avoided. It should be noted that a standard DHW tank has a loss of 15 to 20% per day. The tank is insulated with 60 mm thermal insulation so that the heat losses are reduced to less than 5%. The flow rate of the primary circuit affects the temperature distribution in the storage tank for values between 60 and 240 l/h, beyond the upper value; the temperatures of each unit remain unchanged.

The approach outlined in this experimental protocol is based on a PCM material consisting of a mixture of paraffin wax and sheep fat. The total weight of the mixture is 10 kg, and it is composed of 75% paraffin and 25% sheep fat (Figure 5). This choice is also motivated by the availability of sheep fat which is abundant and free in the region. Paraffin wax is also cheap, which is estimated at a maximum of 270 DZD per kilogram (~1.89 US$/kg) **[37, 38]**. The literature has shown a lack of such studies in the hot-arid regions.

This PCM storage material is incorporated directly on the sidewalls of one of the storage tanks. The mixed PCM was melted using

Preprints (www.preprints.org) | NOT PEER-REVIEWED | Posted: 6 December 2022 doi:10.20944/preprints202212.0095.v1

a flame propane torch and poured into the sides of the storage tank using a large ladle.

Figure 4. Design elements of the storage tanks; the liquefied PCM incorporation in the lateral layers of the storage tank.

The melting phenomenon and the solidification behavior of this new PCM are obtained from differential scanning calorimetry "DSC" measurements. Experimental procedures were conducted in the LGCgE laboratory (School of High Engineering Studies, Lille Campus, France). In Figure 6, the DSC graph shows the relationship between the heat flow and the sample temperature at a heating rate of 1°C/min in the temperature range 10-70°C.

Detailed findings are presented in Table 4. Physical processes of the new PCM take into account the characteristics and thermophysical properties of both substances (fat and paraffin). The melting onset of the new PCM starts at 36.57°C and ends (full melting) at a temperature of 58.39°C (refer to a blue-colored line in Figure 6). The first peak corresponds to the fat melting, while the second peak corresponds to the paraffin melting. The other phase (refer to a red-colored line in Figure 6) indicates that the paraffin solidification starts at a temperature of 59.35°C, whereas the solidification of the sheep fat begins solidification at 51.01°C. The mixing approach made the new PCM ideal for storing heat in DHW applications since the melting and solidification processes occur between 50 and 60°C. The final characteristics of the PCM composite material and its resulting thermophysical properties are summarized in Table 5.

Preprints (www.preprints.org) | NOT PEER-REVIEWED | Posted: 6 December 2022 doi:10.20944/preprints202212.0095.v1

Figure 7 provides a general view of the storage system, including the arrangement of the designed tanks. The storage tank is connected to an electricity network using two precise digital meters. The power supply circuit includes a power-on device in off-peak hours protected by a modular circuit breaker. The two tanks are located so that the incoming water is uniformly distributed to both tanks. Two pressure gauges with an accuracy of 0.01 bar were also installed with shut-off valves to control the water flow. The hydraulic storage connection is ensured by a cold-water inlet and hot water outlet pipes. A pressure reducer to the water heater is added for safety purposes.

Table 4. Analysis results from the unsubtracted heat flow at a heating rate of 1°C/min in the temperature range 10-70 °C.

Phase number	Temperature, in °C		Peak, in °C	Mass enthalpy corresponding to the ΔH reaction, in J/g	Equivalent energy 1 kWh =3600 kJ, in mJ	Reaction type
	At the start of the phase	At the end of the phase				
1	45.05	52.04	51.01	-23.8043	-272.560	The melting point of the sheep fat
2	54.92	62.58	59.35	-34.0144	-389.465	The melting point of the paraffin
3	59.47	56.55	58.39	55.1503	631.470	Paraffin solidification process
4	37.58	35.58	36.57	25.4134	290.984	Solidification point of the sheep fat

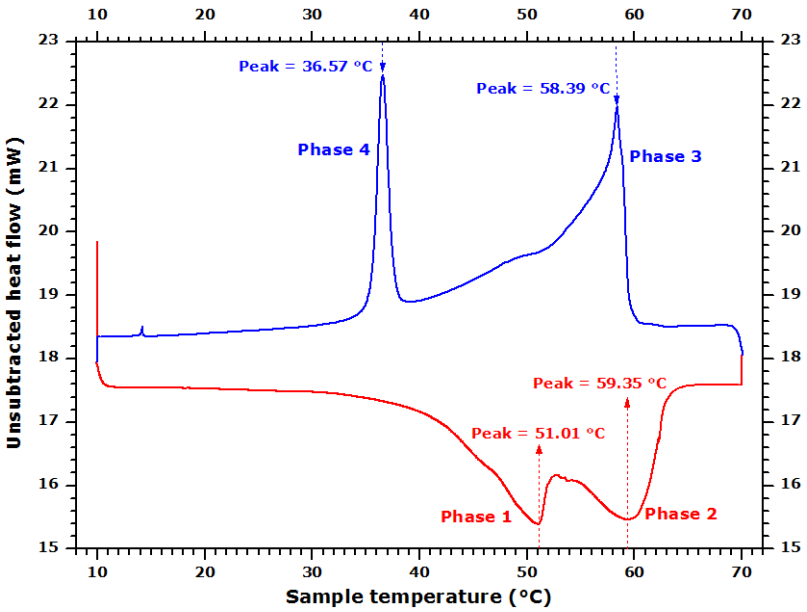

Figure 6. DSC curves for the PCMs mixture (Djeffal et al., 2022)

Table 5. Physical characteristics and technical parameters of the PCM composite material, incorporated in the second storage thank **[37]**

Parameters	Values
Melting temperature	52 °C
Density (solid-state)	920 kg/m^3
Density (liquid-state)	885 kg/m^3
Thermal conductivity (solid-state)	0.215 W/m K
Thermal conductivity (liquid-state)	0.175 W/m K
Latent heat	180-210 kJ/kg

Preprints (www.preprints.org) | NOT PEER-REVIEWED | Posted: 6 December 2022 doi:10.20944/preprints202212.0095.v1

Specific heat (solid-state)	2395 kJ/kg °C
Specific heat (liquid-state)	2451 kJ/kg °C

Experimental works carried out on this MEGASUN solar water heater during the night period have shown that under the effect of generally stable climatic conditions, this prototype will achieve thermal equilibrium. At these times, the flow of water is useless, which is why the circuit will be closed under these conditions. The water temperature inside the storage tank can vary considerably and depending on the degree of solar radiation.

Figure 7. General view of the tanks installation project

3. Energy and financial needs for domestic hot water

3.1. Household's annual hot water demand

The following equation formulates the general term for identifying domestic hot water energy demand **[39]**:

$$Q_{DHW} = p\ 1.1628\ V_{DHW}\ (T_{DHW} - T_{CW}) \quad (5)$$

Q_{DHW}: Energy demand for the hot water production (Wh)
p: Density of the water according to its temperature, and assumed to be equal to 1 kg/liter
V_{DHW}: Required volume of the hot water (per liters)
T_{DHW}: Temperature of the hot water at the draw-off point (°C), a value of 50°C has been assigned.
T_{CW}: The mean temperature of the month's cold water entering the tank or the domestic hot water production coil (instantaneous production), selected values are summarized in Table 6.

Table 6. Monthly and annual energy demand of domestic hot water heating calculated by equation 2, knowing that 1 m³ gas = 1 kWh/10.53 **[39, 40]**

	T_{CW} (°C)	Q_{DHW} (kWh)	Billing invoice from conventional electricity (DZD)	Q_{DHW} (m³ gas)	Billing invoice from natural gas (DZD)
January	09.00	369.48	3 894.32	35.09	
February	09.50	329.65	3 474.55	31.31	**507.46**
March	11.50	346.95	3 656.86	32.95	
April	13.20	320.93	3 382.63	30.48	
May	15.80	308.20	3 248.43	29.27	**483.72**
June	18.50	274.71	2 895.46	26.09	

Preprints (www.preprints.org) | NOT PEER-REVIEWED | Posted: 6 December 2022 doi:10.20944/preprints202212.0095.v1

July	19.30	276.66	2 915.99	26.27	
August	19.10	278.46	2 934.98	26.44	**471.62**
September	18.00	279.07	2 941.42	26.50	
October	15.80	308.20	3 248.43	29.27	
November	12.30	328.78	3 465.36	31.22	**502.97**
December	08.00	378.49	3 989.30	35.94	
Total		**3799.59**	**40 047.72**	**360.83**	**1 965.77**

According to Table 6, and by assuming the above hot water demand, homeowners can provide an annual financial austerity equivalent to about 95.09%. Unfortunately, gas heating also has some disadvantages that can lead to serious operating problems. Gas is flammable, and it is always necessary to ensure that the gas pipes are perfectly sealed to avoid any risk of fire. On the other hand, it is a toxic product and can become lethal if inhaled in large quantities. In addition, poor combustion can also generate carbon monoxide. The gas network and its infrastructure are not supported in several rural and/or urban areas, which adds to the above challenges. In contrast, the advantages of electric water heaters are many, including their ease of installation, generally their low equipment cost, the smooth operation, the elegant design, and the compactness, the adequate environmental safety, and therefore no negative impact on human health.

3.2. Volume and DHW production capacity

Experimental tests were performed under specific initial conditions in which PCMs were in solid-state (removal of accumulated energy). The followed approach is based on the determination of the gain in terms of domestic hot water production expressed as a percentage of energy needs and energy bills in the first case (case of a conventional storage tank). It is well-known that the resulting energy saving depends on a number of parameters such as solar radiation, sunshine duration, sensor surface, tilt angle of the water plate-collector, the orientation of the solar sensor, solar storage volume, the volume of the make-up water, and its geometric, optical, and thermophysical properties. The adopted method led us and therefore required us to guarantee as much as possible the same indoor test conditions (laboratory air temperature around storage tanks, temperature of the cold water at the source, elimination of indoor heat and ventilation sources). The first tests were carried out under specific initial conditions. In the initial state, PCMs are removed from the accumulated energy (solid state).

For the electric water heater, the overall amount of the retained heated water is calculated directly when the temperature of the tank's water reaches the temperature of the selected thermostat. In the case of the hybrid (solar/electric) energy system, the amount of energy required to supply the domestic heating was determined while giving priority to solar energy. The activation of the solar heating system was triggered between 08:10 a.m and 3 p.m, when temperatures reached maximum values. According to these tests, it has been experimentally shown that the resulting water temperatures in both tanks remained consistently below 50 °C. So at this time (at 3 p.m.), our power supply for a fixed thermostat temperature was tripped, it will turn off when we will have water heated to the adjusted desired temperature.

Experiment tests will be carried out for temperatures set at 50, 55, 60, 65, 70, and 75°C. The amount of the produced hot water is then

Preprints (www.preprints.org) | NOT PEER-REVIEWED | Posted: 6 December 2022 doi:10.20944/preprints202212.0095.v1

calculated for each case separately. During the test days in November, the climatic conditions were generally similar and stable (clear sky and low wind speed). The capacity to experimentally produce hot water at 50°C is calculated at the adjusted thermostat temperature, as shown in Figure 8. Additionally, it is possible to draw up prediction curves using the regression method. The regression curves can be used to estimate the effective production capacity of the domestic hot water at 50°C for different water thermostat setpoint. The indicated values lead us thereafter to determine the quantitative gain in terms of domestic hot water production. The results in Figure 8 are based on the solar collector's inclination angle of 51°.

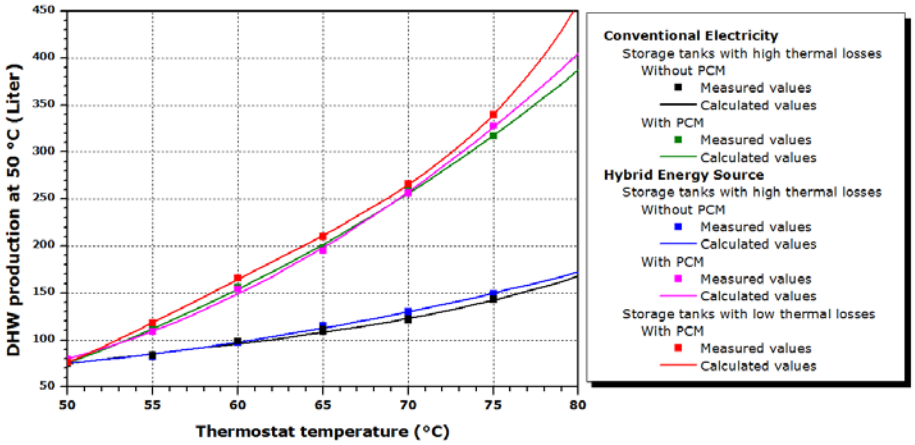

Figure 8. Amount of the produced hot water at 50 °C according to the thermostat temperature

As clear from the figure for all cases, the capacity to produce hot water at 50°C is proportional to the thermostat temperature. As the thermostat setpoint is increased, the hot water produced at 50 °C increases. It is also observed that the integration of PCM into the tank has promoted a considerable increase in the produced hot water compared to the conventional storage tank. At 68.61°C thermostat setpoint, the amount of the produced hot water is doubled when the PCM is used.

Indeed, to calculate the water volume for a conventional tank, resulting values of the mean values relative to the black and blue curves profiles have been used. The same approach is adopted for the PCM-embedded storage tank; resulting values of the mean values relative to the green, pink and red curves profiles have been used. By assimilating the values of the produced hot water capacity to average values, it can be considered that the production of domestic hot water can increase at an estimated rate of 2.96%, 33.06%, 61.03%, 84.94%, 105.46%, 124.66%, and 145.06% for thermostat temperatures set at 50, 65, 70, 75 and 80°C, respectively.

Another important observation is related to the amount of hot water produced at 50 °C, which is found independent of the nature of supply power sources (i.e., electric or hybrid). The figure shows that the produced hot water at 50 °C for the PCM-embedded tanks is almost the same for the electric and the hybrid energy source. For the conventional storage tank with high thermal losses, the difference between the quantities of water heated by electric energy and that from the hybrid energy source (solar energy + electricity energy as a supplement) is, on average, 3.82 liters. The difference between the quantities of water represents, on average, 3.04% compared to the quantity produced by electrical energy and 2.91% compared to that

Preprints (www.preprints.org) | NOT PEER-REVIEWED | Posted: 6 December 2022 doi:10.20944/preprints202212.0095.v1

produced by hybrid energy. This difference represents between 0.03% and 5.77% compared to the amount produced by electrical energy and gradually varies from 0.03% to 5.45% of the produced DHW amount from the hybrid energy source system.

Moreover, in the case of a storage tank with high thermal losses coated by one PCM layer on its sidewall, the difference between the hot water quantities produced by electrical energy and those from the hybrid energy source is on average 5.20 liters. Likewise, the difference between the amount of water is, on average, 2.40% of the quantity produced by electrical energy and 2.38% compared to that produced by hybrid energy. Similarly, this difference which is expressed in liters represents in this case between 0.10% and 6.13% of the quantity produced by electrical energy and between 0.10% and 5.78% of the DHW amount produced by hybrid energy.

In the case of the PCM storage tank, it was noted that the tank with good thermal insulation (i.e., red curve in Figure 8) had provided more hot water production compared with other PCM-embedded tanks with high losses (i.e. pink and green curves in Figure 8).

3.3. Energy cost of the storage tanks with/without PCM using different energy sources

Based on the results, it is possible to deduce that the quantity of hot water is independent of energy sources (i.e., electric or hybrid). Therefore, economic feasibility is deemed important. The electrical energy demand for hot water varies based on the number of occupants and their behavior. The estimated cost for producing one liter of hot water (unit price) at 50 °C was calculated by dividing the electrical power required (measured by the two electric meters) to heat up the volume of the produced hot water. The energy cost is assumed at 10.54 DZD/kWh, knowing that 1 American dollar (US$) = 142.91 Algerian dinar (DZD). The energy cost for the five design cases is shown in Figure 9. The energy cost for water heating is expressed as a function of the thermostat temperature. It is worth mentioning that the solar collector is tilted at 51° which is the optimum tilt angle during the month of testing.

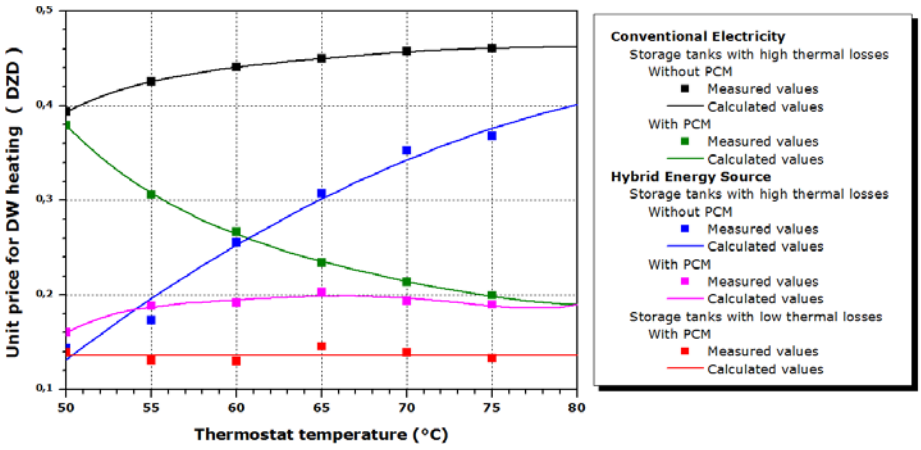

Figure 9. Amount of the produced hot water at 50 °C according to the thermostat temperature

Energy cost of the electrical storage tanks with/without PCMs: Two storage tanks with high thermal losses are using electricity as the main energy source: one without PCM (i.e., the black line in Figure 9) and the other is with PCM (i.e., the green line in Figure 9). The former tank design shows a high energy consumption as the thermostat

 doi:10.20944/preprints202212.0095.v1

setpoint is increased. The poor insulation prevents the water in the tank from staying at the desired temperature. The heating energy consumption has increased by 17.08% when the thermostat setpoint is increased from 50 °C to 75 °C. On the other hand, the PCM-embedded storage tank has positive results. As the thermostat setpoint is increased, the heating energy cost is decreased. For instance, the heating energy cost for the PCM-embedded tank is 3.69% lower than the energy cost of the tank without PCM at 50 °C. The reduction in energy cost is higher at a higher thermostat setpoint. At 80 °C thermostat setpoint, the heating energy cost for the PCM tank is 58.85% lower than the tank without the PCM. Despite the enhanced performance of the PCM-embedded tank compared to the tank without PCM, both tanks designs suffer from high thermal losses. Therefore, thermal insulation should be an integral element in the design of these tanks.

Energy cost of the hybrid (solar/electric) storage tanks with/without PCMs: Three design scenarios are evaluated using a hybrid energy source: high thermal losses tanks with PCM (i.e., the pink line in figure 9) and without PCM (i.e., the blue line in figure 9), and a third design that has low thermal losses with PCM (i.e., the red line in figure 9). The hybrid storage tanks versions have electric heating as a backup, yet solar energy is the default energy source whenever available. The benefit of using PCM is evident for the tanks with a hybrid energy source, as illustrated in figure 9. In particular, the storage tanks with PCM (i.e., the pink and red color lines) show that the energy cost is independent of the thermostat setpoint. The constant difference between these two tanks is due to the thermal insulation, also showing the importance of insulating the tanks. It is also noted that the difference between the electrical and the hybrid PCM-embedded tanks becomes smaller at higher thermostat setpoint. At a higher thermostat setpoint, the use of electrical energy in the hybrid system is becoming dominant over solar energy. On average and beyond 56 °C thermostat setpoint, the hybrid storage tank with high thermal losses and PCM reduced the energy cost by 57.16% compared to the conventional electrical storage tank without PCM.

On the other hand, the energy cost of the tank without the PCM increases as the thermostat setpoint increases. It is also interesting to note that as the thermostat setpoint increases beyond 60°C, the energy cost of the tank without PCM using a hybrid source (i.e., the blue line in Figure 9) is higher than the energy cost of the PCM-embedded tank using electric energy (i.e., the green line in Figure 9), emphasizing the benefits of using PCM for DHW. At 50°C setpoint, the hybrid storage tank (i.e., the blue line in Figure 9) provided 66.55% lower energy cost than the same tank configuration with electric energy (i.e., the black line in Figure 9). This reduction becomes lower as the thermostat setpoint increases until it reaches 13.22% at 80 °C.

In general, the best configuration corresponds to the hybrid heating system with a low heat loss PCM-embedded storage tank that has electrical energy as a backup. The incorporation of these two concepts (PCM+ solar energy) via a well-insulated 80-liter tank resulted in an energy cost reduction between 65.39 and 70.56%. For this option, the energy cost is stabilized at 0.1362 DZD/liter regardless of the thermostat setpoint, as shown in Figure 9.

Preprints (www.preprints.org) | NOT PEER-REVIEWED | Posted: 6 December 2022 doi:10.20944/preprints202212.0095.v1

4. Impact of environmental conditions on the performance of the hybrid PCM-embedded and insulated tank at $T_{Thermostat}$ = 75°C

According to Figure 9, the cost required to electrically heat one liter of stored water in the base case of a high-thermal losses tank (non-isolated storage tank) is estimated at 0.4608 DZD/liter, the integration of the PCM plates in the side walls leads to a reduction of 58.56% in electrical energy cost. In fact, by referring to the hourly data for an entire year, it has been shown that it is possible to project the achieved savings when considering the climatic conditions of the region. The energy savings that will be obtained following the integration of PCMs will therefore not be less than 58.56%.

4.1. Influence of the wind speed

The wind is known to be a prominent factor in convective heat transfer. Hence, the performance of the solar collector may be influenced by the wind speed due to the natural convection. The hybrid PCM-embedded and insulated tank is used to analyze the impact of the wind speeds on the performance of the tank.

For the first trials and during the experiments, the wind speed was measured to be between 12.6 km/h and 18 km/h with an overall clear sky. The experimental results indicated that an energy cost saving of 66.06% was achieved, an additional of 7.5% (66.06% - 58.56%). If the sky is completely clear at the same wind speed range, the wind effect has been slightly less sensitive. The energy cost saving is recorded at least 67.02%, an additional of 8.46% (67.02% - 58.56%).

The performance of this tank was also evaluated when the wind speed was between 4.32 km/h and 12.6 km/h. The results indicated that the tank could achieve energy cost savings of 67.5% and 69.03% for a generally clear sky condition and for a completely clear sky condition, respectively. When the wind speed was greater than 18 km/h, the energy cost savings was 63.06% for an average wind speed that approached 45.86 km/h. These percentages represent the least favorable values adopted after several experimental tests.

4.2. Influence of the solar intensity

The intensity of the received solar radiation depends on the year, the sky cloudiness, the tilt angle of the surfaces, and the site. The sky is generally characterized according to the total cloud cover "N", which is defined as the fraction of the covered sky by all the visible clouds. It is measured in oktas, one okta equal to one-eighth of the celestial vault. It is usually estimated by an observer, sometimes using dark eyeglasses to avoid reflections. However, total cloud cover can be estimated by a measuring instrument for assessing solar radiation components at the horizontal surface. The clarity index "Clar" is expressed in accordance with the following formula **[41]** (CCO, 2022):

$$Clar\,(\%) = 100\,(1 - N) \qquad N = \sqrt{1.4286\,\frac{E_{diffus}}{E_{global}} - 0.3} \tag{6}$$

E_{global} and E_{diffus} represent global horizontal and diffuse solar radiations (Wm^{-2}), respectively. It is likely to have a sunny, veiled, cloudy, or overcast sky, but it is possible to have different intensities for the same type of sky. Veiled skies can be observed in the cirrostratus cloud's presence. In general, the appearance of the veiled sky will be in the milky form due to these clouds, which are extended but not very thick, and it is possible to see the sun through them. For instance, if the

Preprints (www.preprints.org) | NOT PEER-REVIEWED | Posted: 6 December 2022 doi:10.20944/preprints202212.0095.v1

city of Conflans-en-Jarnisy which is located in the north of Meurthe, and Moselle in the center of Lorraine in France, a classification according to two radically different periods can be assigned. The site is at a latitude of 49.1667°, a longitude of 5.85°, a minimum altitude of 185 m, a maximum of 226 m, and an average of about 200 meters. Summer (June 21) and winter (December 21) solstices were retained as examples (Table 7) **[41, 42]**.

For the same total cloud cover, a drastic fall in daily irradiation due to the year season can be obtained. For this case, it is extreme and near 84.92%. In order to achieve our own predictions, the experimental classification must therefore be carried out in accordance with the solar radiation intensity reflected by the daily solar irradiation. A series of experimental tests, which are a renewal of the same previous protocol but with other external weather conditions, allowed us to suggest the results of Table 8.

Table 7. Classification of the sky type according to the total cloud cover, case of the city of Conflans-en-Jarnisy **[42]**

Sky state	Summer solstice (June 21)			Winter solstice (December 21)		
	Solar radiation peak (at 12 TSV) W/m²	Daily irradiation Wh/m²	Total cloud cover Oktas	Solar radiation peak (at 12 TSV) W/m²	Daily irradiation Wh/m²	Total cloud cover Oktas
Sunny	Between 940.30 and 1012.30	Between 8397.84 and 9040.63	Between 0 and 0.0711	Between 250.10 and 269.20	Between 1266.54 and 1363.19	Between 0 and 0.0709
Veiled	Between 726.80 and 940.30	Between 6486.47 and 8397.84	Between 0.0711 and 0.2825	Between 193.30 and 250.10	Between 978.84 and 1266.54	Between 0.0709 and 0.2820
Cloudy	Between 530.10 and 726.80	Between 4734.22 and 6486.47	Between 0.2825 and 0.4763	Between 141.00 and 193.30	Between 714.31 and 978.84	Between 0.2820 and 0.4760
Overcast	Less than 530.10	Less than 4734.22	More than 0.4763	Less than 141.00	Less than 714.31	More than 0.4760

Table 8. Financial savings from test experiments according to the daily solar radiation intensity

Daily irradiations (kWh/m²)		Less than 1.75 m/s (1)	Between 1.75 and 3.11 m/s (2)	Between 3.11 and 4.15 m/s (3)	Between 4.15 and 4.98 m/s (4)	Between 4.98 and 5.39 m/s (5)	Between 5.39 and 5.74 m/s (6)	More than 5.74 m/s (7)
Retained values according to the wind speed	**Less than 4.32 km/h (1)**	On average 59.99 %	61.50 %	65.06 %	67.01 %	69.72 %	81.98 %	93.27 %
	Between 4.32 and 12.6 km/h (2)	On average 59.09 %	60.53 %	62.98 %	66.44 %	68.10 %	78.05 %	85.70 %
	Between 12.6 and 18 km/h (3)	On average 58.83 %	59.82 %	61.00 %	63.05 %	66.96 %	72.22 %	80.66 %
	More than 18 km/h (4)	On average 58.66%	58.90 %	60.08 %	62.37 %	64.16 %	68.29 %	75.34 %

The saving rate of financial needs, therefore, depends heavily on this intensity. For each case, at least three tests under almost equivalent solar irradiations and generally at the same wind speeds were carried out; the least attractive value will be retained. Taking the sky subjected to solar irradiation between 6.53 and 6.87 kWh and a low wind speed (less than 4.32 km/h) as an application example, four tests following the same experimental protocol have shown that the financial savings were 72.62%, 69.72%, 71.5%, and 69.99%. The value of 69.72% has been assigned. The intensity of the sun's radiation received on the ground depends on the site, the inclination angle, and the sky state. Suppose all conditions are unfavorable (very high wind speed and very low solar intensity). In that case, the effect of the whole concept (PCM + solar energy) will be limited to only the PCM effect; the financial saving

Preprints (www.preprints.org) | NOT PEER-REVIEWED | Posted: 6 December 2022 doi:10.20944/preprints202212.0095.v1

equivalent to a thermostat temperature of 75°C cannot be below 59.50%.

4.3. Forecast and projected operating results

Following these experimental results, a figure can be drawn up, which includes real and predicted values of the financial savings achieved by using a hybrid solar/electric system containing a low heat loss PCM storage tank. In Figure 10, the values correspond to the minimum percentages from several experimental tests for the same conditions. The methodology has allowed us to ensure that the obtained financial savings are undoubtedly consistent and reliable. These values may be more interesting (slightly higher) than those of the selected values, but it is not possible to have values below these retained values. The non-linear regression functions are in the curve adjustments form.

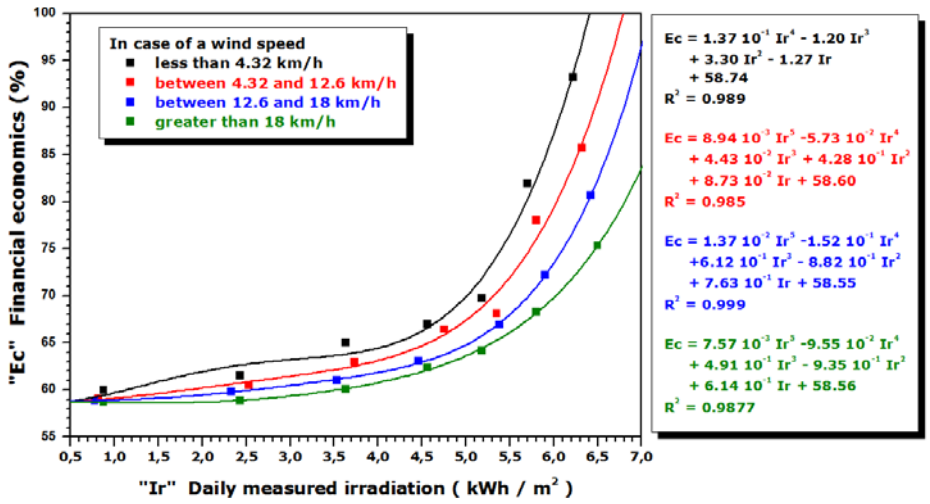

Figure 10. Prediction of financial savings based on solar radiation intensity and wind speed

In contrast to the solar intensity and the wind speed, the effect of the outside ambient air temperature on financial savings is generally very small. Using the results obtained from Figure 10, and on the basis of the curves of the representative climatic conditions represented by Figures 11, 12, and 13, the results can be generalized to the annual basis as outlined in Table 9. This database was collected from the radiometric station of the Ghardaïa research unit **[43, 44]**.

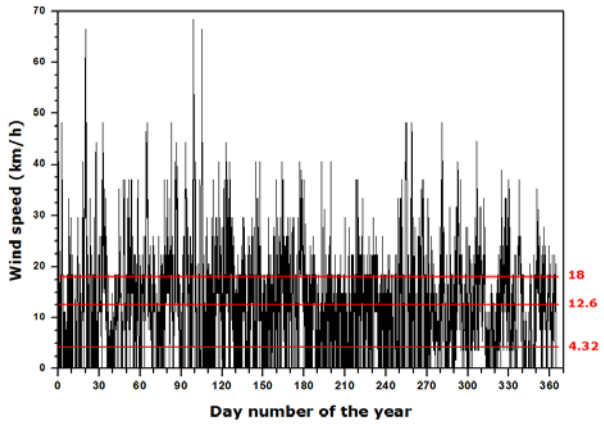

Figure 11. Variation of the wind speed

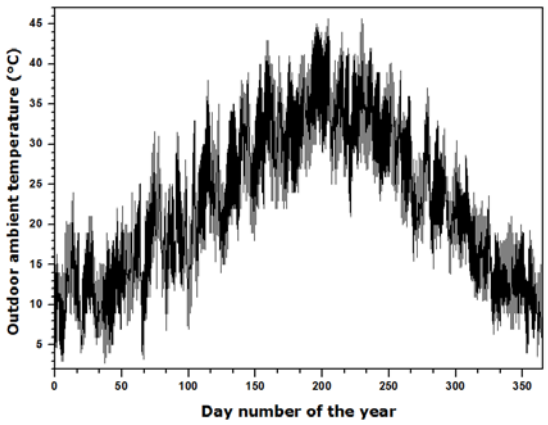

Figure 12. Variation of the ambient temperature

To achieve the best energy cost savings, it is desirable to convert the horizontal solar irradiations to the solar irradiations incident on

Preprints (www.preprints.org) | NOT PEER-REVIEWED | Posted: 6 December 2022 doi:10.20944/preprints202212.0095.v1

surfaces at an optimal tilt, which may vary from month to month, as shown in Table 9. The values were determined using the Perrin de Brichambaut approach **[43, 39]**. This method allowed us to draw on Figure 13 the extreme values corresponding to the optimum inclination for the totally clear sky (black lines) and the already indicated values for the edges of solar irradiations.

The database indicates that the Ghardaïa climate is a desert climate with mild and very cold winters at night and very hot and sunny summers. Sky conditions and radiation are clear for much of the year, but winds are frequent.

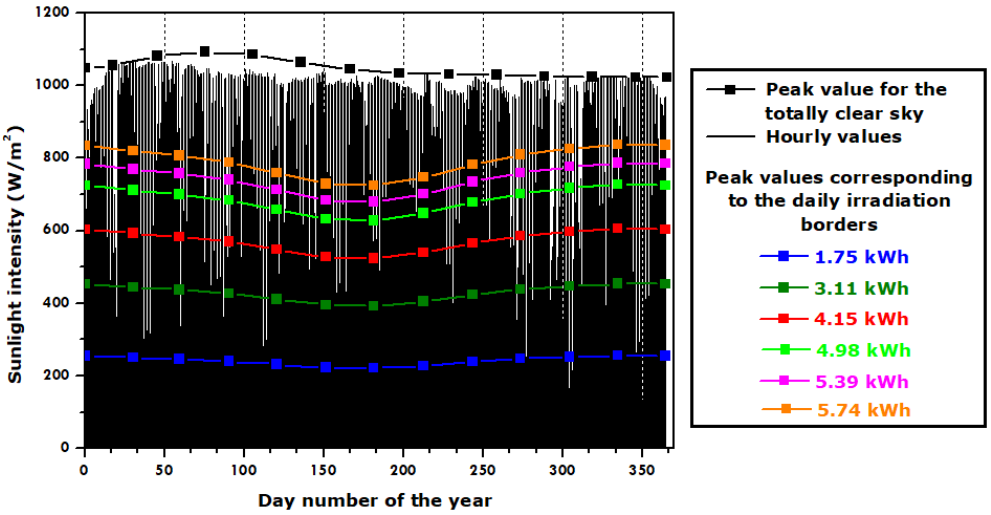

Figure 13. Peak borders and intensity of the sun's radiation at the optimum tilt angle

The equivalent savings for each month in Table 9 is calculated using the following relationship:

$$Equivalent\ \ savings\ \ = \frac{\sum_{i=1}^{n} Number\ \ of\ \ days_i\ \ \ Potentiel\ \ savings_i}{Total\ \ number\ \ of\ days} \qquad (7)$$

Where i: the number of the case, n: is the total number of cases, total number of days = 365.

According to Table 9, the annual average clarity index is estimated to be 86.58%. Indeed, by adopting the average optimum inclination of the surface on a monthly basis, the potential yearly average savings of at least 80.25% may be achieved. The wind speed will reveal the difference in the expected monthly savings if the monthly average of the daily irradiation inclined at the monthly average of the optimal tilt angle is globally close and stable. The most suitable months are those characterized by a high solar intensity reflected by an optimized receiving surface and a fairly low average daily wind speed compared to other months. In this case, financial savings may exceed 80%. In the months of July, August, September, and December, the average savings are 84.45%, 83.81%, 83.65%, and 82.64%, respectively.

However, it should be noted that despite the drop in average daily irradiations to 5.58 kWh/day in December, the saving rate always remains important due to the average daily wind speed, which is clearly low during this month. The main drawback of a flat plate collector is its front convective heat loss which is significant at high wind speeds. The second weakness of the flat collector in the winter is that it requires a better inclination; this situation sometimes creates a more difficult configuration to implement.

Preprints (www.preprints.org) | NOT PEER-REVIEWED | Posted: 6 December 2022 doi:10.20944/preprints202212.0095.v1

The addressed objective was to firstly recovering PCM material and using them as an alternative raw material that can be reintegrated into DHW heating process. Furthermore, if the annual DHW electrical needs correspond to a consumption of 3799.5943kWh/year (equivalent to 250 liters of hot water per day), the annual bill to be paid (10.54 DZD per kWh) is therefore 40 047.72 DZD per year. If the hybrid-energy heating system is used, the cost of heating the water is 0.1362 DZD per litre under clear skies. This case is valid at 86.58% (316 days) for the entire year. The other days (for sky of any type) correspond at least to the worst case (totally overcast sky, case of a PCM tank with low heat loss) which relates to an invoice of 0.2 DZD per liter. The installation therefore results in a reduction in annual requirements of almost 67%. (0.1362 DZD x 250 litres x 316days) + (0.2 DZD x 250 litres x 49 days) = 13 209.8 DZD.

Table 9. Financial savings to be achieved using the hybrid system

	Clarity index calculated by equation 6 (%)	Monthly average of the optimal tilt angle (°)	Monthly average of the daily irradiation inclined at the monthly average of the optimal tilt angle (Wh/Day)		Wind speed (km/hour)			General remarks		Expected minimum potential savings compared to the first case (%)	
			Calculation results Totally clear sky	Measurement values	Min	Moy	Max	Case numbers according to Table 8	Number of days for cases	Per day	Equivalent savings
January	79.56	52.44	7321.22	5824.46	0.00	11.14	66.60	(7)-(4) (7)-(3) (7)-(2) (7)-(1) (4)-(4) (3)-(4)	12 12 04 01 01 01	75.34 80.66 85.70 93.27 62.37 60.08	78.40
February	84.64	44.84	7644.60	6470.45	0.00	14.20	48.24	(7)-(4) (7)-(3) (7)-(2)	13 11 4	75.34 80.66 85.70	78.91
March	83.12	34.22	7856.45	6530.28	0.00	15.06	48.24	(7)-(4) (7)-(3) (7)-(2) (7)-(1) (6)-(3) (5)-(3) (4)-(2)	18 6 3 1 1 1 1	75.34 80.66 85.70 93.27 72.22 66.96 66.44	77.29
April	88.60	23.03	8039.41	7122.81	0.00	15.13	68.40	(7)-(4) (7)-(3) (7)-.2 (7)-(1)	20 7 2 1	75.34 80.66 85.70 93.27	77.87
May	88.80	14.24	8240.45	7325.80	0.00	13.79	44.28	(7)-(4) (7)-(3) (7)-(2) (5)-(4)	11 11 7 2	75.34 80.66 85.70 64.16	78.84
June	93.58	10.10	8216.04	7688.69	0.00	14.74	40.68	(7)-(4) (7)-(3) (7)-(2)	12 17 1	75.34 80.66 85.70	78.70
July	95.43	11.89	8096.50	7726.22	0.00	7.82	40.68	(7)-(4) (7)-(3) (7)-(2) (7)-(1)	3 9 14 5	75.34 80.66 85.70 93.27	84.45
August	93.83	19.10	7740.25	7262.90	0.00	11.50	37.08	(7)-(4) (7)-(3) (7)-(2) (7)-(1)	2 12 14 3	75.34 80.66 85.70 93.27	83.81
September	87.28	29.49	7415.00	6472.22	0.00	11.37	48.24	(3)-(4) (3)-(3) (7)-(4) (7)-(3) (7)-(2) (7)-(1)	1 1 4 6 10 8	60.08 61.00 75.34 80.66 85.70 93.27	83.65
October	83.75	40.71	7192.20	6023.36	0.00	12.73	48.24	(7)-(4) (7)-(3) (7)-(2) (7)-(1) (6)-(4) (5)-(3) (3)-(2) (3)-(4)	6 10 9 1 1 1 1 2	75.34 80.66 85.70 93.27 68.29 66.96 62.98 60.08	78.76
November	80.55	50.05	7029.75	5662.52	0.00	13.36	44.64	(7)-(4) (7)-(3) (7)-(2)	9 5 9	75.34 80.66 85.70	79.50

Preprints (www.preprints.org) | NOT PEER-REVIEWED | Posted: 6 December 2022 doi:10.20944/preprints202212.0095.v1

								(7)-(1) (6)-(4) (4)-(3) (3)-(4) (3)-(3)	3 1 1 1 1	93.27 68.29 63.05 60.08 61.00	
December	79.77	54.60	6999.28	5583.58	0.00	11.24	37.08	(7)-(4) (7)-(3) (7)-(2) (7)-(1) (5)-(2)	6 12 6 6 1	75.34 80.66 85.70 93.27 68.10	82.64

5. Conclusion

The electric water heater is one of the simplest solutions for DHW application, but it consumes a significant amount of energy and requires regular maintenance. By installing a customized solar water heater in a sunny region, it can present a better alternative since it uses clean and inexhaustible energy. However, solar may also be intermittent during the day. Phase change materials (PCMs) have shown the potential to elongate the use of solar energy as well as flatten the supply of energy. In this context, two hot water storage tanks were installed in a laboratory setting: a conventional storage tank without PCMs and a PCMs-embedded tank without thermal insulation.

A novel PCMs mixture composed of 75% paraffin and 25% sheep fat was developed for this purpose, which has a melting temperature between 35.58°C and 62.58°C, making it an ideal option for this application. The tanks were heated either using electrical energy or hybrid energy (solar and electricity). The PCM-embedded tank was then thermally enhanced with thermal insulation to reduce the thermal losses.

The experimental results indicated that the best configuration corresponds to the hybrid heating system containing an insulated PCM-embedded storage tank. Regardless of the thermostat setpoints, the energy cost was stabilized around 0.1362 DZD/liter (i.e., 0.00096 US$/liter) of hot water. The energy cost savings ranged between 65.39 and 70.56% (on average 69.26%) compared to the conventional hot water storage tank. On an annual basis, this novel tank configuration may achieve an average energy cost savings of 80.25% when the tilt of the flat plate solar collector is optimized on a monthly basis. In case of insufficient sunlight, the heat is produced by a backup electrical heater.

A further enhancement of this configuration may be achieved by using vacuum tubes solar collectors to reduce the convective heat transfer that could be dominant in flat plate collectors.

Reference

1. ATE, 2022. Agence de la transition écologique L'eau chaude sanitaire. [Online]. Available https://www.ademe.fr/expertises/batiment/passer-a-laction/elements-dequipement/leau-chaude-sanitaire (Accessed September 2022).
2. Ruble, I.; Khoury, P.El. Lebanon's market for domestic solar water heaters: Achievements and barriers. *Energy for Sustainable Development* **2013**, 17, 54-61.
3. Hohne, P.A.; Kusakana, K.; Numbi, B.P. A review of water heating technologies: An application to the South African context. *Energy Reports* **2019**, 5, 1-19.
4. Kumar, R.; Rosen, M.A. Thermal performance of integrated collector storage solar water heater with corrugated absorber surface. *Applied Thermal Engineering* **2010**, 13, 1764-1768.
5. Kontopoulos, E.; Martinopoulos, G.; Lazarou, D.; Bassiliades, N. An ontology-based decision support tool for optimizing domestic solar hot water system selection. *Journal of Cleaner Production* **2016**, 112(5), 4636-4646.

6. Kee, S.Y.; Munusamy, Y.; Ong, K.S. Review of solar water heaters incorporating solid-liquid organic phase change materials as thermal storage. *Applied Thermal Engineering* **2018**, 131, 455-471.
7. Da Silva, F.A.S.; Dezan, D.J.; Pantaleão, A.V.; Salviano, L.O. Longitudinal vortex generator applied to heat transfer enhancement of a flat plate solar water heater. *Applied Thermal Engineering* **2019**, 158, 113790.
8. Wang, L.; Zheng, D.; Cheng, G. An adaptability evaluation of large-scale solar energy for hot water application based on energy-economic-environment consideration: A case study of city-residential buildings in China. *Journal of Cleaner Production* **2021**, 296, 126585
9. Paul, R. Scoping Study for Residential Water Heaters Mapping and Benchmarking Project. Technical Report by Weide 2014.
10. Catherine, Q.; Wheeler, J.; Wilkinson, R.; De Jager, G. Hot water usage profiling to improve geyser efficiency. *Journal of Energy in Southern Africa* **2012**, 23(1), 39-45.
11. Hepbasli, A.; Kalinci, Y. A review of heat pump water heating systems. *Renewable and Sustainable Energy Reviews* **2009**, 13(6-7), 1211-1229.
12. Cholewa, T.; Siuta-Olcha, A.; Anasiewicz, R. On the possibilities to increase energy efficiency of domestic hot water preparation systems in existing buildings - Long term field research. *Journal of Cleaner Production* **2019**, 217, 194-203.
13. Fanney, A.H.; Dougherty, B.P. The thermal performance of residential electric water heaters subjected to various off-peak schedules. *Journal of Solar Energy Engineering* **1996**, 118(2), 73-80.
14. Jiang, Y.; Yang, X. China's urban residential building energy consumption analysis. *City & House* **2008**, 78-79.
15. Zhang, L.; Gudmundsson, O.; Eric Thorsen, J.; Li, H.; Svendsen, S. Optimization of China's centralized domestic hot water system by applying Danish elements. *Energy Procedia* **2014**, 61, 2833-2840.
16. Liang, Z.; Zheng, Y.; Zhou, N.; Liu, S. User research-based design strategy for an electric water heater and its application. IOP Conf. Series: *Materials Science and Engineering* **2019**, 573, 012052.
17. Tan, Z.Q.; Yang, J.J.; Lou, Z.B.; Wei, C.J. Design of intelligent home electric water heater control system. *Instrumentation Technology* **2016**, 3, 1-4.
18. Dong, L. Research on customer satisfaction of electric water heater installation service based on structural equation model. Master Thesis, Tianjin University of Finance and Economics, 2017.
19. Mostafaeipour, A.; Zarezade, M.; Goudarzi, H.; Rezaei-Shouroki, M.; Qolipour, M. Investigating the factors on using the solar water heaters for dry arid regions: A case study. *Renewable and Sustainable Energy Reviews* **2017**, 78, 157-166.
20. Hohne, P.A.; Kusakana, K.; Numbi, B.P. Techno-economic comparison of timer and optimal switching control applied to hybrid solar electric water heaters. International Conference on the Industrial and Commercial Use of Energy (ICUE) 2018, 13-15, 1-6.
21. Kim, Y.; Zhang, Q. Economic and environmental life cycle assessments of solar water heaters applied to aquaculture in the US. *Aquaculture* **2018**. 495, 44-54.
22. Shi, J.; Lin, K.; Chen, Z.; Shi, H. Annual dynamic thermal performance of solar water heaters: A case study in China's Jiangsu province. *Energy and Buildings* **2018**, 173, 399-408.
23. Urmee, T.; Walker, E.; Bahri, P.A.; Baverstock, G.; Rezvani, S.; Saman, W. Solar water heaters uptake in Australia - Issues and barriers. Sustainable Energy Technologies and *Assessments* **2018**, 30, 11-23.
24. Harmim, A.; Boukar, M.; Amar, M.; Haida, A. Simulation and experimentation of an integrated collector storage solar water heater designed for integration into building façade. *Energy* **2019**. 166, 59-71.
25. Almeshaal, M.; Arunprasad, V.; Palaniappan, M.; Kolsi, L. Experimental study of a solar water heater fitted with spacer at the leading edge of Left-Right screw tapes. *Case Studies in Thermal Engineering* **2020**, 22, 100777.
26. Mandal, S.K.; Kumar, S.; Singh, P.K.; Mishra, S.K.; Singh, D.K. Performance investigation of nanocomposite based solar water heater. *Energy* **2020**, 198, 117295.
27. Manoj Kumar, P.; Mylsamy, K. A comprehensive study on thermal storage characteristics of nano-CeO_2 embedded phase change material and its influence on the performance of evacuated tube solar water heater. *Renewable Energy* **2020**, 162, 662-676.

28. Naidoo, A. The socio-economic impacts of solar water heaters compared across two communities: A case study of Cato Manor. Renewable and Sustainable Energy Reviews 2020, 119, 109525.
29. Touabaa, O.; Ait Cheikh, M.S.; Slimani, M.A.; Bouraiou, A.; Ziane, A.; Necaibia, A.; Harmim, A. Experimental investigation of solar water heater equipped with a solar collector using waste oil as absorber and working fluid. *Solar Energy* **2020**, 199, 630-644.
30. Siampour, L.; Vahdatpour, S.; Jahangiri, M.; Mostafaeipour, A.; Goli, A.; Shamsabadi, A.A.; Atabani, A. Techno-enviro assessment and ranking of Turkey for use of home-scale solar water heaters. *Sustainable Energy Technologies and Assessments* **2021**, 43, 100948.
31. Lafri, D.; Hamid, A.; Belhamel, M.; Semmar, D. Study of the thermal behaviour of a solar heat exchanger storage tank (in French). *Journal of Renewable Energies* **2001**, 127-132.
32. Bekkouche, S.M.A. Thermal behaviour Modelling of some solar devices. Doctoral Thesis in Physical Sciences at the Sciences Faculty of Abou Bekr Belkaïd University, Tlemcen, 2008.
33. Rahimpour, M.R.; Kazerooni, N.M.; Parhoudeh, M. Water Treatment by Renewable Energy-Driven Membrane Distillation, Current Trends and Future Developments on (Bio) Membranes. *Renewable Energy Integrated with Membrane Operations* **2019**. Chapter 8, 179-211.
34. Abu-Hamdeh, N.H.; Khoshaim, A.; Alzahrani, M.A.; Hatamleh, R.I. Study of the flat plate solar collector's efficiency for sustainable and renewable energy management in a building by a phase change material: Containing paraffin-wax/Graphene and Paraffin-wax/graphene oxide carbon-based fluids. *Journal of Building Engineering* **2022**, 57(1), 104804.
35. Koholé, Y.W.; Fohagui, F.C.V.; Tchuen, G. Flat-plate solar collector thermal performance assessment via energy, exergy and irreversibility analysis. *Energy, Conversion and Management* **2022**, X 15, 100247.
36. Salem, T. Integration of active solar thermal components in the built structure (in French). Doctoral Thesis in Civil Engineering, National Institute of Applied Sciences, Lyon, 2007.
37. Djeffal, R.; Cherier, M.K.; Bekkouche, S.M.A.; Younsi, Z.; Hamdani, M.; Al-Saadi, S. Concept development and experimentation of a Phase Change Material (PCM) enhanced domestic hot water. *Journal of Energy Storage* **2022**, 51, 104400.
38. Djeffal, R. Latent heat storage efficiency, experimentation and application to real energy systems (in French). Doctoral Thesis in Renewable Energies, University of Ferhat Abbas Setif 1, Algeria, 2021.
39. Bensaha, A. Exploitation of renewable energy sources for a sustainable building design in an isolated and semi-arid Algerian site (in French). Doctoral Thesis in Electronics, Option: Renewable Materials and Energies, Amar Telidji University of Laghouat, Algeria, 2021.
40. Belgherras, S.; Bekkouche, S.M.A.; Benouaz, T.; Benamrane, N. Prospective analysis of the energy efficiency in a farm studio under Saharan weather conditions. *Energy and Buildings* **2017**, 145, 342-353.
41. CCC, 2022. Cloudiness or clouds cover (in French). [Online]. Available https://www.monsite-meteo.eu/PC/G-HC-Nebulosite.php. Accessed December 2022.
42. CCO, 2022. Cloud - Cloudiness and Opacity (in French). [Online]. Available https://fr.wikipedia.org/wiki/Nuage. Accessed December 2022.
43. Hamdani, M.; Bekkouche, S.M.A.; T. Benouaz; Cherier, M.K. A new modelling approach of a multizone building to assess the influence of building orientation in Saharan climate. *Thermal Science* **2015**, 19(2), 591-601.
44. Cherier, M.K. Passive use of solar energy in Ghardaïa buildings (in French). Doctoral Thesis in Renewable Energies, Abou Bekr Belkaid University of Tlemcen, Algeria, 2018.